

# Detailed Topography of the Fermi Surface of $\text{Sr}_2\text{RuO}_4$

C. Bergemann,<sup>1</sup> S. R. Julian,<sup>1</sup> A. P. Mackenzie,<sup>2</sup> S. NishiZaki,<sup>3</sup> and Y. Maeno<sup>3,4</sup>

<sup>1</sup>*Cavendish Laboratory, University of Cambridge, Madingley Road, Cambridge CB3 0HE, United Kingdom*

<sup>2</sup>*School of Physics and Astronomy, University of Birmingham, Edgbaston, Birmingham B15 2TT, United Kingdom*

<sup>3</sup>*Department of Physics, Graduate School of Science, Kyoto University, Kyoto 606-8502, Japan*

<sup>4</sup>*CREST, Japan Science and Technology Corporation, Kawaguchi, Saitama 332-0012, Japan*

(Submitted to Physical Review Letters on 3 September 1999)

We apply a novel analysis of the field and angle dependence of the quantum-oscillatory amplitudes in the unconventional superconductor  $\text{Sr}_2\text{RuO}_4$  to map its Fermi surface (FS) in unprecedented detail, and to obtain previously inaccessible information on the band dispersion. The three quasi-2D FS sheets not only exhibit very diverse magnitudes of warping, but also entirely different dominant warping *symmetries*. We use the data to reassess recent results on *c*-axis transport phenomena.

PACS numbers: 71.18.+y, 71.27.+a, 74.25.Jb

The layered perovskite oxide  $\text{Sr}_2\text{RuO}_4$  has attracted considerable experimental and theoretical attention since the discovery of superconductivity in this compound five years ago [1]. Fermi liquid behaviour of several bulk transport and thermodynamic properties was observed in early work [1,2], and the existence of mass enhanced fermionic quasiparticles was demonstrated explicitly by the observation of quantum oscillations in the magnetization (de Haas-van Alphen or dHvA effect) and resistivity [3]. Quantitative similarities between the Fermi liquid in  $^3\text{He}$  and that in  $\text{Sr}_2\text{RuO}_4$  hint at the possibility of p-wave superconducting pairing [4]. Evidence supporting such a scenario has come from the existence of a very strong impurity effect [5], a temperature independent Knight shift into the superconducting state [6], a muon spin rotation study indicating broken time reversal symmetry [7] and a number of other experiments [8,9]. Taken together, these favour spin triplet superconductivity with a p-wave vector order parameter and a nodeless energy gap.

$\text{Sr}_2\text{RuO}_4$  appears to be an ideal material in which to investigate unconventional superconductivity in real depth: of all known compounds exhibiting this phenomenon,  $\text{Sr}_2\text{RuO}_4$  offers the best prospects of a complete understanding of the normal state properties within standard Fermi liquid theory [10]. This would provide a solid foundation for all theoretical models. It has become clear, however, that further progress will require very detailed knowledge of the electronic structure of  $\text{Sr}_2\text{RuO}_4$ . For example, one of the most successful current theories relies on the assumption that the FS consists of two sheets derived from bands with strong Ru  $d_{xz,yz}$  character and one with strong Ru  $d_{xy}$  character [11]. These are supposed to form weakly coupled subsystems with very different pairing interactions [12]. This theory has successfully predicted non-hexagonal vortex lattice structures [13,14], but it is less clear whether, in its simplest form, it will provide a satisfactory explanation for recent measurements of the temperature dependence of the density of normal excitations in the superconducting state [15].

Of central importance to the understanding of

$\text{Sr}_2\text{RuO}_4$  is the origin of the quasiparticle mass enhancement and how it relates to magnetic fluctuations. Recent observations of cyclotron resonances [16] give the promise of separating the various contributions to the enhancement, but identifying the type of resonance and the extent to which electron interactions are affecting the observed masses requires more detailed knowledge of the Fermi surface than has been available to date. Clues to the magnetic fluctuation spectrum have come from nuclear magnetic resonance [17] and neutron scattering experiments [18] and from calculations [19]. Both ferro- and antiferromagnetic fluctuations appear to be present, the latter due to nesting of the FS. Angular dependent magnetoresistance oscillations (AMRO) can give information about the in-plane topography of the FS and the extent to which it is nested. However, with three bands crossing the Fermi level, the interpretation of AMRO data on  $\text{Sr}_2\text{RuO}_4$  [20] has been somewhat ambiguous.

Progress on all the issues discussed above requires high resolution, sheet-by-sheet knowledge of the FS of  $\text{Sr}_2\text{RuO}_4$ . As shown in previous studies [3], the dHvA effect is ideally suited to this, as data from individual FS sheets can be identified without ambiguity. For this reason, we have performed a comprehensive angular dHvA study in  $\text{Sr}_2\text{RuO}_4$ . Full analysis of the data required extension and generalisation of previously reported theoretical treatments [21] of dHvA in nearly 2D materials. As a result, we present an unprecedentedly detailed picture of the warping of each FS sheet. A series of recent measurements of *c*-axis transport phenomena are discussed in light of the full experimentally determined dispersion.

Quantum-oscillatory effects in a crystal arise from the quantization of the cyclotron motion of the charge carriers in a magnetic field  $\mathbf{B}$ . For three-dimensional metals, only the extremal cyclotron orbits in  $\mathbf{k}$ -space lead to a macroscopic magnetization, and the quantitative treatment has been known for decades [22].

For a quasi-2D metal, the FS consists of weakly corrugated cylinders. While such weak distortions have little effect on the cross-sectional areas which determine the

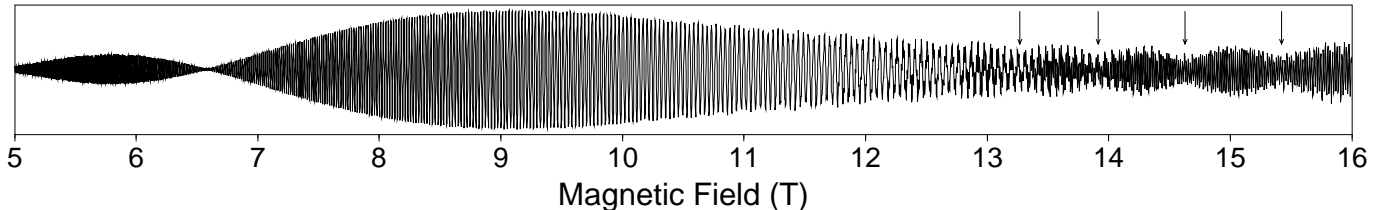


FIG. 1. Example of a dHvA field sweep on  $\text{Sr}_2\text{RuO}_4$ , for  $\theta = 9.8^\circ$  off the  $c$ -axis in the  $[001] \rightarrow [110]$  rotation study. The vertical axis is the pick-up signal (in arbitrary units) at the second harmonic of the excitation frequency. At high fields, beats in the  $\beta$ -oscillations are visible, as indicated by arrows.

dHvA frequency, they still affect the interference of the magnetization contributions of different parts of the FS and therefore lead to a characteristic amplitude reduction. Conversely, as we will show, analysis of the experimental dHvA amplitude behaviour can reveal fine details of the topography of the underlying Fermi cylinders.

In the most basic case, a simple corrugation of the Fermi cylinder leads to a beating pattern in the magnetization. Analysis of the beats for on-axis fields gives some information about the *magnitude* of the warping, but further conclusions have to rely on assumptions about the precise form of the corrugation [3]. At the next level of approximation, the FS dispersion can be determined within the traditional scope of the Yama $\acute{c}$ ji effect [21,23]. A preliminary attempt to extract information on  $\text{Sr}_2\text{RuO}_4$  in this way, however, has not achieved agreement between the data and the predictions of the simple model [24]. We show that a much more extensive treatment is needed that (a) considers Fermi cylinder corrugation of arbitrary shape and (b) if necessary, goes beyond the extremal orbit approximation. Also, to extract meaningful information from experiments, one needs data of much higher quality than has been available to date.

In the following, we will briefly present the results of a full quantitative treatment of the oscillatory magnetization for a Fermi cylinder that is warped arbitrarily but still compliant with the Brillouin zone (BZ) symmetry of  $\text{Sr}_2\text{RuO}_4$ ; details will be presented elsewhere [25]. It is convenient to parameterize the corrugation of the cylinder through an expansion of the local Fermi wavevector,

$$k_F(\phi, \kappa) = \sum_{\substack{\mu, \nu \geq 0 \\ \mu \text{ even}}} k_{\mu\nu} \cos \nu\kappa \begin{cases} \cos \mu\phi & (\mu \bmod 4 \equiv 0) \\ \sin \mu\phi & (\mu \bmod 4 \equiv 2) \end{cases} \quad (1)$$

(see Table I for illustration). Here,  $\kappa = ck_z/2$  where  $c$  is the height of the body-centered tetragonal unit cell, and  $\phi$  is the azimuthal angle of  $\mathbf{k}$  in the  $(k_x, k_y)$ -plane. The  $\beta$ - and  $\gamma$ -cylinders are centered in the BZ; symmetry allows nonzero  $k_{\mu\nu}$  only for  $\mu$  divisible by 4. The  $\alpha$ -cylinder runs along the corners of the BZ and has nonzero  $k_{\mu\nu}$  only for  $\nu$  even and  $\mu$  divisible by 4, or for  $\nu$  odd and  $\mu \bmod 4 \equiv 2$ . The average Fermi wavevector is given by  $k_{00}$ , which is assumed to be much larger than the higher-order  $k_{\mu\nu}$ .

One also has to consider the effect of the magnetic field:

spin-splitting drives the spin-up and spin-down surfaces apart; the parameters  $k_{\mu\nu}$  can be taken to expand weakly and linearly in the field as in  $k_{\mu\nu}^{\uparrow\downarrow} = k_{\mu\nu} \pm \chi_{\mu\nu}B$ . Ordinary spin-splitting is described by  $\chi_{00}$  alone, while higher-order contributions would correspond to the underlying electronic band structure being flatter at some points on the Fermi surface than at others. Indeed, this anomalous spin-splitting will prove essential for describing the  $\alpha$ -sheet in  $\text{Sr}_2\text{RuO}_4$ .

If a magnetic field is applied at polar and azimuthal angles  $\theta$  and  $\phi$ , the Fermi surface cross-sectional area perpendicular to the field which cuts the cylinder axis at  $\kappa$  is given by the Bessel function expansion

$$a^{\uparrow\downarrow}(\kappa) = \frac{2\pi k_{00}}{\cos \theta} \sum_{\substack{\mu, \nu \geq 0 \\ \mu \text{ even}}} (k_{\mu\nu} \pm \chi_{\mu\nu}B) \quad (2) \\ \times J_\mu(\nu\kappa_F \tan \theta) \cos \nu\kappa \begin{cases} \cos \mu\phi & (\mu \bmod 4 \equiv 0) \\ -\sin \mu\phi & (\mu \bmod 4 \equiv 2) \end{cases}$$

which is a generalization of Yama $\acute{c}$ ji's earlier treatment [21]; here,  $\kappa_F = ck_{00}/2$ . The total quantum oscillatory magnetization now arises from the interference of the individual contributions of the cylinder cross-sections; at constant chemical potential, the fundamental component of the oscillations is given by

$$\tilde{M} \propto \sum_{\uparrow\downarrow} \int_0^{2\pi} d\kappa \sin \left( \frac{\hbar a^{\uparrow\downarrow}(\kappa)}{eB} \right). \quad (3)$$

Eqs. (2) and (3) describe oscillations at the undistorted frequency  $\hbar k_{00}^2/2e \cos \theta$ , with a characteristic amplitude modulation induced by the interference. One can thus infer the warping parameters  $k_{\mu\nu}$  by modeling experimentally obtained amplitude data [26].

We have performed a thorough dHvA rotation study in the  $[001] \rightarrow [110]$  plane on a high-quality crystal of  $\text{Sr}_2\text{RuO}_4$  with  $T_c > 1.3$  K. The experiments were carried out on a low noise superconducting magnet system in field sweeps from 16 T to 5 T, at temperatures of 50 mK. A modulation field of 5.4 mT amplitude was applied to the grounded sample, and the second harmonic of the voltage induced at a pick-up coil around the sample was recorded, essentially measuring  $\partial^2 M/\partial B^2$ , with well-established extra contributions from the field modulation, impurity scattering, and thermal smearing [22].

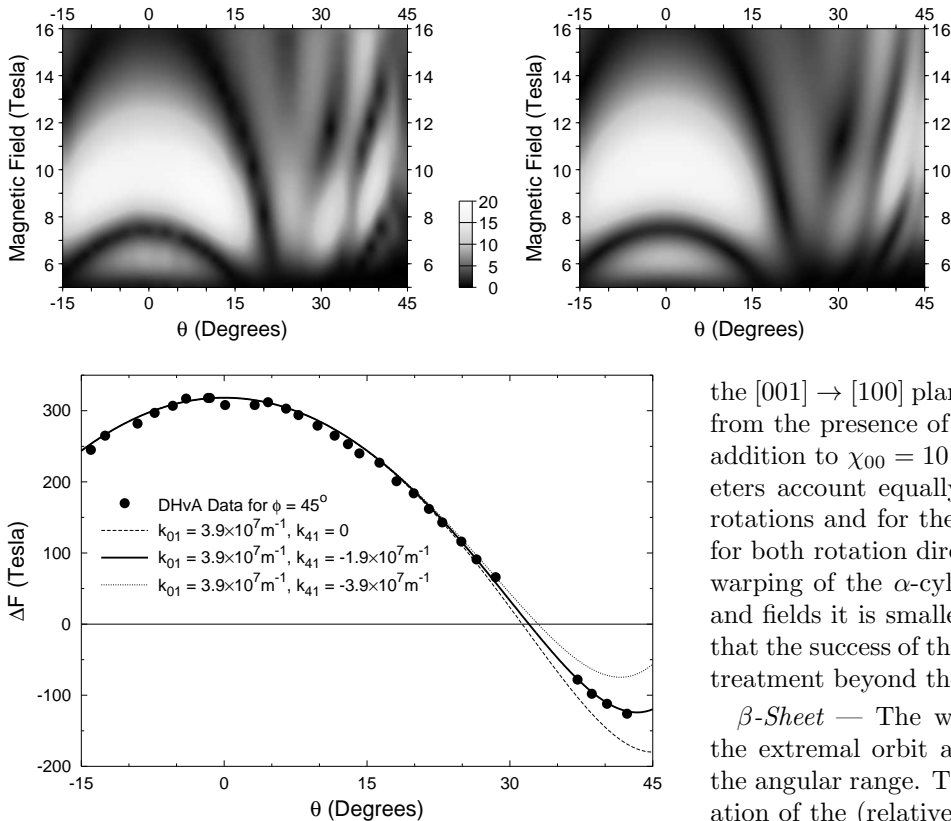


FIG. 3. Angular dependence of the beat frequency of the  $\beta$ -oscillations in  $\text{Sr}_2\text{RuO}_4$  (cf. Fig. 1) in the  $[001] \rightarrow [110]$  rotation study (full circles).  $\Delta F(0^\circ)$  fixes  $k_{01}$  at  $3.9 \times 10^7 \text{ m}^{-1}$ ; the data are compared against the predicted behaviour for cylindrically symmetric warping (dashed line), for zero dispersion along the BZ axes (dotted line), and for  $k_{04}$  as tabulated in Table I (solid line).

A typical signal trace, demonstrating the high quality of our data, can be viewed in Fig. 1. Overall, 35 such sweeps were performed, at angular intervals of  $2^\circ$ . For each of the dHvA frequencies corresponding to the three FS sheets, we have extracted the local dHvA amplitude through filtering in the Fourier domain. The dHvA amplitude can then be visualized versus magnitude and direction of the field, as shown in the density plot in Fig. 2 for the  $\alpha$ -sheet. We have also performed similar data analysis for a second extensive rotation study of short high-field (18 T to 15 T) sweeps in the  $[001] \rightarrow [100]$  plane; these runs used a different sample. We now turn to the results of the analysis for all three FS sheets, where Table I presents the deduced values for the  $k_{\mu\nu}$ .

$\alpha$ -Sheet — The most striking features of the data in Fig. 2 are qualitative differences with similar data in the  $[001] \rightarrow [100]$  plane (Ref. [24] and the present study), and the absence of spin-zeroes that should be visible as vertical black lines. We are able to account for both effects, and produce near-perfect agreement with experiments as seen by comparing the two panels of Fig. 2, using the  $k_{\mu\nu}$  as given in Table I. The dominant  $k_{21}$ -term affects the dHvA amplitude for  $\phi = 45^\circ$  but has no effect for fields in

FIG. 2. Density plot of the dHvA amplitude (in arbitrary units) of the  $\alpha$ -frequency in  $\text{Sr}_2\text{RuO}_4$ , in the experimental  $[001] \rightarrow [110]$  rotation study (left), and comparison with the theoretical simulation, using the warping parameters in Table I (right). The theoretical calculation incorporates experimental effects such as the field modulation amplitude characteristic.

the  $[001] \rightarrow [100]$  plane. The absence of spin-zeroes arises from the presence of a finite  $\chi_{21} \simeq -5 \times 10^5 \text{ m}^{-1}\text{T}^{-1}$  in addition to  $\chi_{00} = 10.4 \times 10^5 \text{ m}^{-1}\text{T}^{-1}$ . The same parameters account equally well for data from  $[001] \rightarrow [100]$  rotations and for the amplitude of the second harmonic for both rotation directions. It should be noted that the warping of the  $\alpha$ -cylinder is so weak — at some angles and fields it is smaller than the Landau level spacing — that the success of the model requires the use of our exact treatment beyond the extremal orbit approximation.

$\beta$ -Sheet — The warping is comparatively large, and the extremal orbit approximation is valid over most of the angular range. The Yamaji angle of  $32^\circ$  and the variation of the (relatively fast) beating frequency  $\Delta F$  with  $\theta$  (Fig. 3) reveal that the dominant warping parameters are  $k_{01}$  and  $k_{41}$ , as tabulated in Table I. They have opposite signs, so the  $c$ -axis dispersion is *largest along the zone diagonals*. It is difficult to extract meaningful information on the higher-order terms, but we believe that the data set an upper bound for a double warping contribution of  $|k_{02}| < 10^7 \text{ m}^{-1}$ . The spin-splitting behaviour is intricate, and while it is certain that higher-order  $\chi_{\mu\nu}$  are needed to explain the data, it is impossible at this stage to extract them without ambiguity.

$\gamma$ -Sheet — Due to stronger impurity damping, the  $\gamma$ -signal is only observable at fields of more than 13 T. Along  $[001] \rightarrow [110]$ , its amplitude peaks at  $\theta = \pm 13.7^\circ$ , implying that the dominant corrugation is *double warping*, i.e.  $k_{02} \gg k_{01}$ . We obtained a rough estimate of its strength from the *sharpness* of this amplitude maximum — it is difficult to assess  $k_{02}$  from an on-axis beating pattern, as that cannot be established in the short field range over which  $\gamma$ -oscillations are visible. For the  $[001] \rightarrow [100]$  rotation, the amplitude maximum occurs at  $\theta = 14.6^\circ$ . The deviation of the two measured  $\theta$ -values from each other and from the simple Yamaji prediction of  $14.1^\circ$  yields  $k_{42}$ , whose sign implies that the  $c$ -axis dispersion is *largest along the zone axes*. At present, it is not possible to extract reliable information on the spin-splitting parameters.

To the order of expansion given here, it is possible to calculate the contribution of each FS to the  $c$ -axis conductivity. The  $\beta$ -sheet dominates with a 86% share, compared to 8% for the  $\alpha$ - and 6% for the  $\gamma$ -sheet. This provides new insight into recent AMRO experiments by

TABLE I. Summary of the extracted warping parameters  $k_{\mu\nu}$  (in units of  $10^7 \text{ m}^{-1}$ ) of the three FS sheets of  $\text{Sr}_2\text{RuO}_4$  [26]. Entries symbolized by a long dash are forbidden by the BZ symmetry. The first row visualizes the warping for the different values of  $\mu$  and  $\nu$ , on top of a large  $k_{00}$ .

	$k_{00}$	$k_{01}$	$k_{02}$	$k_{21}$	$k_{41}$	$k_{42}$
$\alpha$	304.7	—	0.33	1.3	—	-1.0
$\beta$	623	3.9	small	—	-1.9	small
$\gamma$	754	small	0.5	—	small	0.3

Ohmichi *et al.* [20] as it strongly suggests that the AMRO signal originates predominantly from the  $\beta$ -sheet (rather than the  $\alpha$ -sheet as had previously been assumed). The AMRO data then fix the “squareness” parameter of the  $\beta$ -cylinder as  $k_{40} = 5.3 \times 10^8 \text{ m}^{-1}$ , giving quantitative information about the FS nesting on that sheet.

Our work also helps to clarify the interpretation of absorption spectra in cyclotron resonance [16], which have recently been used to assess quasiparticle mass enhancements in  $\text{Sr}_2\text{RuO}_4$ . The “periodic orbit resonance” geometry used in those experiments assesses modulations in the  $c$ -axis Fermi velocity. The strongest signals from such resonances in their simplest form should again stem from the  $\beta$ -sheet, and the unusual warping symmetry would lead to dominant resonances at  $4\omega_c, 8\omega_c, \dots$  for the  $\beta$ - and  $\gamma$ -orbits, and at  $2\omega_c, 4\omega_c, \dots$  for the  $\alpha$ -orbit.

High-precision dHvA itself can provide normally inaccessible information on spin-dependent many-body effects, by measuring both the specific heat and the spin susceptibility mass enhancements. For the  $\alpha$ -sheet, we have  $m^*/m = 3.4$  and  $m_{\text{susc}}^*/m = 4.1$ , the latter obtained from spin-splitting analysis assuming  $g \simeq 2$ . We would expect the ratio  $m_{\text{susc}}^*/m^*$  to diverge at a ferromagnetic quantum critical point; the small ratio here suggests that, at least for the  $\alpha$ -sheet, the paramagnetic susceptibility enhancement is matched by specific heat contributions from phonons or large- $q$  spin fluctuations [10,18].

Finally, an intriguing feature of the present study is the qualitative difference between the dominant warping symmetries observed for the three FS sheets of  $\text{Sr}_2\text{RuO}_4$ . Detailed comparison with the results of band structure calculations would be very informative to test the accuracy of these computations for the weak out-of-plane dispersions in quasi-2D metals in general. For  $\text{Sr}_2\text{RuO}_4$  in particular, this would also be a check on the commonly made assignment of the Ru  $d_{xz,yz}$  orbital character to the  $\alpha$ - and  $\beta$ -sheets, and the  $d_{xy}$  character to the  $\gamma$ -sheet, which lies at the foundation of theories of orbital dependent superconductivity.

In summary, the full analysis of angle-dependent dHvA amplitude data has emerged as an extremely powerful tool to determine the exact topography of the FS in quasi-2D metals. We have been able to extract quantitative in-

formation on the corrugation of all three Fermi cylinders of  $\text{Sr}_2\text{RuO}_4$ . The single warping of the  $\beta$ -sheet provides most of the  $c$ -axis dispersion, while the ellipsoidal warping of the  $\alpha$ - and the double warping of the  $\gamma$ -sheet are less significant.

We wish to thank S. Hill, E. M. Forgan, A. J. Schofield, G. J. McMullan, and G. G. Lonzarich for stimulating and fruitful discussions. The work was partly funded by the U.K. EPSRC. C.B. acknowledges the financial support of Trinity College, Cambridge; and A.P.M. gratefully acknowledges the support of the Royal Society.

- [1] Y. Maeno *et al.*, Nature **372**, 532 (1994).
- [2] Y. Maeno *et al.*, J. Phys. Soc. Jpn. **66**, 1405 (1997).
- [3] A. P. Mackenzie *et al.*, Phys. Rev. Lett. **76**, 3786 (1996); the correct quasiparticle masses are given in A. P. Mackenzie *et al.*, J. Phys. Soc. Jpn. **67**, 385 (1998).
- [4] T. M. Rice and M. Sigrist, J. Phys.: Condens. Mat. **7**, 643 (1995).
- [5] A. P. Mackenzie *et al.*, Phys. Rev. Lett. **80**, 161 (1998).
- [6] K. Ishida *et al.*, Nature **396**, 658 (1998).
- [7] G. M. Luke *et al.*, Nature **394**, 558 (1998).
- [8] K. Ishida *et al.*, Phys. Rev. B **56**, 505 (1997).
- [9] R. Jin *et al.*, Phys. Rev. B **59**, 4433 (1999); C. Honerkamp and M. Sigrist, Prog. Theor. Phys. **100**, 53 (1998).
- [10] S. R. Julian *et al.*, Physica B **261**, 928 (1999).
- [11] T. Oguchi, Phys. Rev. B **51**, 1385 (1995).
- [12] D. F. Agterberg, T. M. Rice, and M. Sigrist, Phys. Rev. Lett. **78**, 3374 (1997).
- [13] D. F. Agterberg, Phys. Rev. Lett. **80**, 5184 (1998).
- [14] T. M. Riseman *et al.*, Nature **396**, 242 (1998).
- [15] S. NishiZaki, Y. Maeno, and Z. Q. Mao, in Proceedings of the International Conference on Physics and Chemistry of Molecular and Oxide Superconductors, Stockholm, July 1999 (unpublished).
- [16] S. Hill *et al.*, cond-mat/9905147; J. Singleton, private communication.
- [17] T. Imai *et al.*, Phys. Rev. Lett. **81**, 3006 (1998); H. Mukuda *et al.*, J. Phys. Soc. Jpn. **67**, 3945 (1998).
- [18] Y. Sidis *et al.*, cond-mat/9904348.
- [19] I. I. Mazin and D. J. Singh, Phys. Rev. Lett. **79**, 733 (1997).
- [20] E. Ohmichi *et al.*, Phys. Rev. B **59**, 7263 (1999).
- [21] K. Yamaji, J. Phys. Soc. Jpn. **58**, 1520 (1989).
- [22] See for example D. Shoenberg, *Magnetic Oscillations in Metals* (Cambridge University Press, 1984).
- [23] See for example J. Wosnitza, *Fermi Surfaces of Low-Dimensional Organic Metals and Superconductors* (Springer, Berlin, 1996).
- [24] Y. Yoshida *et al.*, J. Phys. Soc. Jpn. **67**, 1677 (1998).
- [25] C. Bergemann *et al.*, in preparation.
- [26] The dHvA effect is insensitive to  $k_{\mu 0}$  for  $\mu > 0$ ; these parameters can only be probed by other methods such as AMRO. Ambiguities can also arise for the *sign* of the  $k_{\mu\nu}$ : while the average Fermi wavevector  $k_{00}$  and the spin-splitting  $\chi_{00}$  must be positive, the dHvA amplitude is invariant under a simultaneous sign change of the other  $k_{\mu\nu}$  and  $\chi_{\mu\nu}$  for either all  $\nu$ , or all even  $\nu$ , or all odd  $\nu$ .